A Kinetic Monte Carlo Model for Stochastic Switching in Monolayer MoS_2 RRAMs

Lavanya Peddaboina[1*], Piyush Kumar[1*], Oves Badami[1], Shubhadeep Bhattacharjee[1#]
[1]*Electrical Engineering, Indian Institute of Technology, Hyderabad, Sangareddy, 502284,*
*Equal Contributions #Email: shubhadeep@ee.iith.ac.in / Phone: +91 40 2301 6481

***Abstract*— We construct a kinetic Monte Carlo (kMC) model to simulate the impact of stochastic multi-hotspot chalcogen-mediated switching on the *I-V* characteristics and associated variability in monolayer MoS_2 RRAMs. The designed physics-informed rate equations capture the abrupt and gradual (with electric field) SET and RESET, respectively and enable the extraction of key material parameters. The calibrated model yields an excellent fit with experimental *I-V* and replicates the large cycle-to-cycle (C2C) variability (coefficient of variance, $\sigma/\mu > 0.5$). Next, we examine the controlled annihilation of hotspots in the RESET process, using DC and pulsed biasing schemes - thereby tuning the statistical parameters of HRS variability at runtime. The change in the mean ($\mu \sim 30 - 600$ MΩ) and coefficient of variance ($\sigma/\mu \sim 1 - 4$) in HRS variability obtained by tuning the stop voltage in the RESET cycle (V_{stop}) is limited. However, the pulsed biasing scheme allows a much larger control over ($\mu \sim 10^3$ to 10^9 Ω) and ($\sigma/\mu \sim 10^{-2}$ to 10^1), by adjusting the pulse height (V_p), duration (t_{pw}), and number of pulses (N_p). Finally, the promise of these devices as tunable stochastic sources is illustrated using a *n:n (n=8-256)* challenge response pair (CRP) based physically unclonable function (PUF). These PUFs demonstrate state-of-the-art inter- and intra-Hamming distance, and the degree of stochasticity is validated using Shannon entropy and NIST SP 800-22 tests.**

Keywords*— *Kinetic Monte Carlo, Stochastic switching, monolayer 2D Materials, RRAM, Tunable Statistics, Physically Unclonable Functions, Shannon Entropy, NIST SP 800-22.

I. Introduction

The development of area-scalable, low-power solid-state devices for true random number generation is crucial for hardware realization of security, cryptography, and authentication applications. Presently, the stochastic sources used in true random number generators (TRNGs) rely on inherent physical randomness introduced during manufacturing, such as transistor mismatches, process variations, and structural defects. These characteristics of these devices cannot be altered post-fabrication and offer limited variability, which can lead to biased or correlated random numbers, thereby compromising the unpredictability of the generated random number bitstream [1]. Therefore, the development of devices that exhibit large and run-time tunable cycle-to-cycle (C2C) variability would open new vistas.

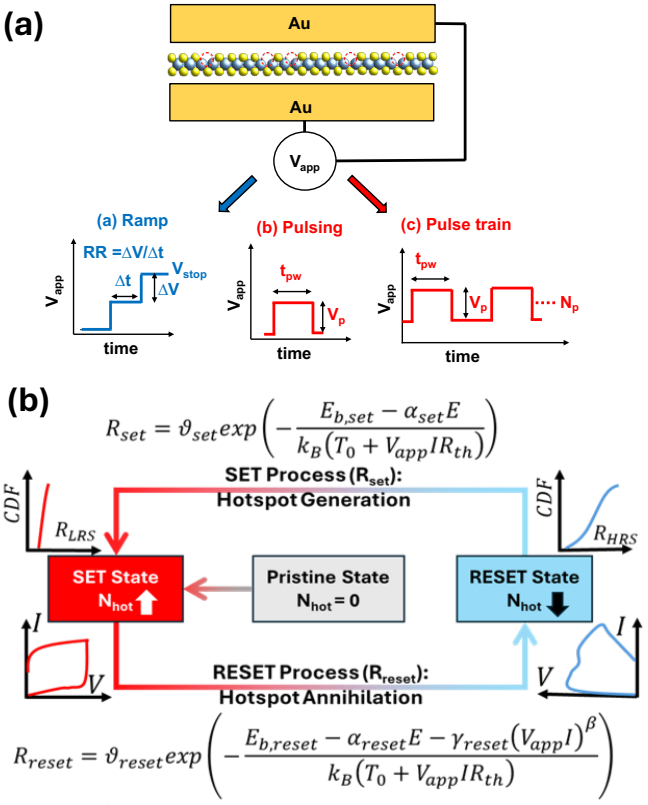

Fig.1 Device and simulation methodology (a) Monolayer MoS_2 RRAM device under DC ramp and pulse biasing (b) Kinetic Monte Carlo (kMC) simulation methodology used in this work illustrating transitions between pristine, SET and RESET states and associated rate equations.

Two-terminal solid-state devices based on a metal–insulator–metal (MIM) structure, commonly known as resistive random-access memory (RRAM), exhibit switching mechanism that relies on the formation and rupture of conductive filaments between two metal electrodes. Generally, the variability in such systems arises from the size and shape of the filaments created in successive operational cycles [2]. In conventional RRAM, the insulating layer is typically an oxide material. In these devices, the formation and rupture of one or a few conductive filament(s), enable the device's resistive switching mechanism. This limits the range and tunability of the statistical distribution parameters of

variability. In RRAMs, where a 2D material is sandwiched between two metal electrodes, the switching mechanism is inherently different from that in oxide-based RRAMs. Resistive switching, for example, in monolayer MoS_2-based RRAMs is mediated by numerous sulfur vacancies (~1 million defects in a 2×2 μm² area) that are present on its basal plane [3]. Under an applied bias, these defects can transform into conductive hotspots. Since there are a large number of such filaments that can independently 'turn on/off' in successive SET/RESET cycles – the range of variability that these devices exhibit is also sizeable [4].

In this work, we simulate the sulfur-vacancy-mediated stochastic formation (SET) and annihilation (RESET) of hotspots in monolayer MoS_2 RRAMs. This stochastic switching mechanism leads to variability in the *I–V* characteristics. First, by employing physics-informed rate equations in our kinetic Monte Carlo (kMC) model, we accurately capture the abrupt SET and gradual RESET behaviour in RRAM, achieving excellent calibration with experimental *I–V* data. This enables the extraction of key material parameters for further simulations. Next, we use the calibrated model to generate cycle-to-cycle (C2C) variability in the *I–V* characteristics over consecutive SET and RESET cycles. The statistical parameters mean(μ) and coefficient of variance(σ/μ) of variability in the gradual RESET process can be tuned over several orders of magnitude by varying the stop voltage (V_{stop}) for DC ramp biasing, and the pulse amplitude (V_p), duration (t_{pw}), and number of pulses (N_p) for single-pulse and pulse train biasing. Finally, we demonstrate the implementation of a physically unclonable function (PUF) using our devices.

II. Device Schematic and Simulation Methodology

The RRAM under consideration is a monolayer of MoS_2 with S-vacancies (marked with red circles) sandwiched between two inert (Au) electrodes [Fig.1(a)]. The device is subjected to three biasing schemes: DC ramp (blue) and single pulse, pulse train (red), as illustrated in [Fig.1(a)]. We employ the kinetic Monte Carlo (kMC) methodology to simulate the device characteristics and the associated C2C variability arising due to stochastic formation (SET) and annihilation (RESET) of conductive hotspots. In the kMC model, we employ a physics-informed rate equation that describes abrupt SET and gradual RESET as detailed in [Fig.1(b)] [4].

During the SET process, as the applied voltage (V_{app}) increases, the corresponding rise in the electric field (E) exponentially enhances the probability of overcoming the formation barrier ($E_{b,set}$), leading to the abrupt formation of hotspots at a critical electric field. This causes a sharp reduction in the resistance, and the device switches from the high-resistance state (HRS) to the low-resistance state (LRS) [Fig. 2(a)]. During the RESET process, the device transitions from the LRS to HRS. As the applied bias voltage (V_{app}) increases, it causes a rise in current (I), leading to an increase in device temperature due to Joule heating. To capture this effect, the RESET rate equation is modified to include a Joule heating term $\gamma_{reset}(V_{app}\cdot I)^{\beta}$. The increased temperature lowers the energy barrier for hotspot annihilation ($E_{b,reset}$) and gradually assists in the annihilation of conductive hotspots, driving the device back into the high-resistance state (HRS). The denominator of the exponent in both rate equations captures the increase in current (I) with applied voltage (V_{app}), which leads to a rise in lattice temperature. This temperature increase is modeled using the net thermal resistance (R_{th}), the value of R_{th} decreases as the number of hotspots increases. The parameters ϑ_{set} and ϑ_{reset} represent the attempt frequencies for a sulfur vacancy transforming into a conductive hotspot (SET) and for the annihilation of hotspot (RESET), respectively. The material parameters used in the rate equations mentioned in [Fig.1(b)] are extracted by calibration with experimental data as shown in [Fig. 2(a)][4].

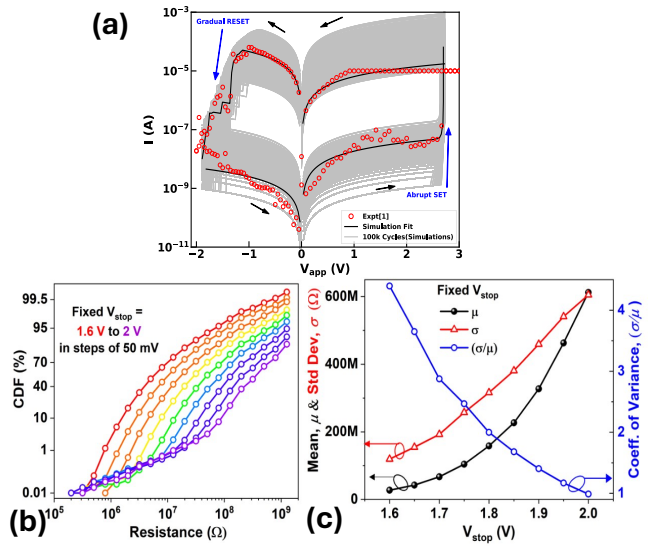

Fig.2 Calibration, C2C variability, and tunability of HRS variability statistics under DC ramp biasing. (a) Calibration with experimental data and C2C variability in the I-V characteristics for both HRS and LRS. (b) CDF (%) demonstrating tunability of HRS statistics with DC biasing by varying V_{stop}. (c) Statistical parameters mean (μ), standard deviation (σ), and coefficient of variance (σ/μ) for fixed V_{stop}.

III. Device Characteristics and Variability

First, we evaluate the device characteristics with DC biasing. [Fig.2(a)] demonstrates an excellent match of our simulations (black line) with the experimental data (red open symbols)[4,5]. Furthermore, 10k SET and RESET cycles generated using the calibrated model are shown using silver lines [Fig.2(a)], where, despite a large distribution in HRS and LRS resistances, a sizeable memory window (10^2) is evident. The C2C variability in the device is due to the unpredictability of the number and location of hotspots at the end of each set/reset cycle. Next, we leverage the gradual RESET characteristics of the device to tune the variability statistics by varying the maximum biasing voltage during the RESET

process, also referred to as stop voltage (V_{stop}). The cumulative distribution function (CDF%) for each V_{stop}, ranging from −1.6 V to −2.0 V in 50 mV increments, is shown in Fig. 2(b). The CDF% of HRS shifts toward higher resistance values, indicating an increase in the mean (μ) of the distribution with increasing V_{stop}. This is because, due to the gradual RESET process, the number of hotspots that get annihilated on an average increase with V_{stop}. Also, we observe that while the absolute value of the standard deviation increases with V_{stop}, the normalized variability or the coefficient of variance (σ/μ), decreases with V_{stop}. This is because with higher V_{stop} nearly all the (finite) hotspots available for conduction annihilate, which caps/saturates the normalized variability of the HRS state.

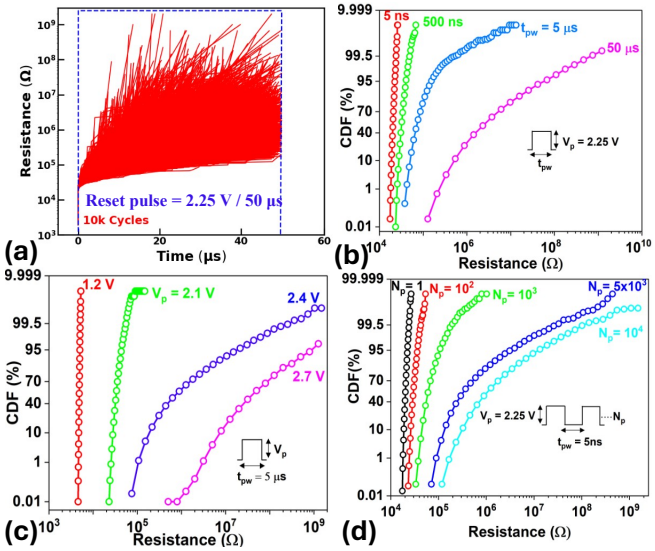

Fig.3 Variability statistics with pulse and pulse train biasing schemes. (a) Resistance vs. time illustrating C2C HRS variability under pulse biasing with fixed pulse height (V_P) and duration (t_{pw}). The CDF% curves of HRS under pulse biasing by (b) varying t_{pw} (fixed V_P), (c) varying V_P (fixed t_{pw}), and (d) varying number of pulses N_p (fixed V_P & t_{pw}).

Second, we explore the pulsed biasing scheme to modulate the C2C variability in HRS resistance. The evolution of the HRS as a function of time when the device is subjected to a pulse height (V_p) of 2.25 V and a pulse duration (t_{pw}) of 50 µs over 10k cycles of operation is shown in [Fig 3(a)]. A resistance range spanning ~ 5 orders of magnitude (10^4 to 10^9 Ω) is observed for 10k cycles, indicating significantly higher variability compared to DC biasing conditions. The statistical parameters associated with this HRS variability can be further tuned using three scenarios (1) varying t_{pw} (with fixed V_p = 2.25 V) [Fig.3(b)], (2) varying V_p (with fixed t_{pw} = 5 µs) [Fig.3(c)], and (3) varying the number of pulses, N_p (for fixed V_p = 2.25 V, t_{pw} = 5 ns) [Fig.3(d)] as demonstrated in CDF (%) plots. With increasing pulse parameter values (V_p, t_{pw}, N_p), the CDF (%) curves shift toward higher resistance values. As a result, the mean and the coefficient of variation (CV) of the HRS initially increase. For larger pulse parameters, the mean begins to saturate, and the CV decreases, as shown in [Fig.4(a-d)]. This behaviour is similar to that seen in DC biasing conditions, where with higher V_p, t_{pw} and/or N_p, nearly all the (finite) number of hotspots are annihilated, which drives the system toward more repeated resistance states. [Fig.4(a–d)] demonstrates by varying pulse parameters the mean (μ) and the coefficient of variance (σ/μ) can be tuned over six (10^3 to 10^9) and three (10^{-2} to 10^1) orders of magnitude, respectively. As evident in Fig 4(b,d), the normalised variability (σ/μ), has an optimal V_p which yields the maximum variability for fixed t_{pw} and N_p, below which the majority of the hotspots are active (not annihilated) and above which most hotspots tend to get annihilated. The value of this optimal V_p is inversely correlated to the magnitude of fixed t_{pw} and N_p as evident in Fig. 4 (b,d)]. These plots predict the optimal operating conditions to maximize/minimize variability for appropriate applications.

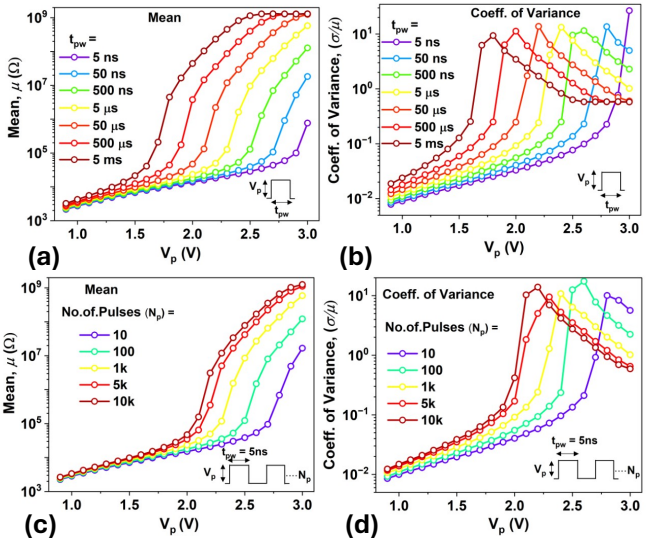

Fig.4 Tunability of HRS variability statistics with pulse biasing. Statistical parameters of HRS resistance:(a) Mean and (b) coefficient of variance by varying V_p and t_{pw} (fixed N_p), and (c) Mean and (d) coefficient of variance by varying V_p and N_p (fixed t_{pw}).

IV. MoS_2 RRAM – Based Physically Unclonable Functions (PUFs)

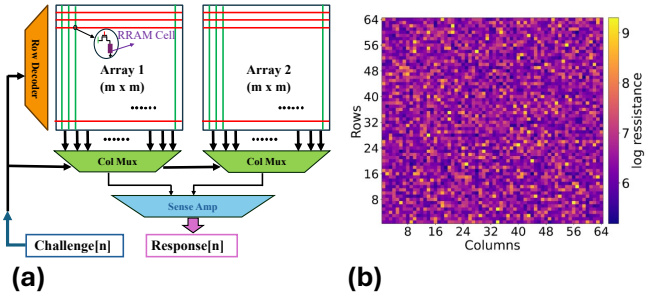

Fig.5 *(a) PUF architecture for n:n CRP using two 1T-1R MoS_2 RRAM arrays; (b) Resistance distribution across the array cells.*

Physically unclonable functions (PUFs) rely on devices exhibiting inherent randomness in their characteristics. In this context, our MoS_2-based RRAM devices offer a unique solution with large statistical control with biasing parameters. To evaluate the same, we construct a PUF architecture [Fig. 5(a)] with *n:n* challenge response pairs (CRPs). The resistance distribution across the memory array, where all the cells are initially set in the HRS is illustrated in Fig. 5(b). A common challenge is applied to the two arrays initialized with HRS

resistances, and the corresponding memory cells are selected. The resistance values of these selected cells are then compared. If the resistance of a cell in Memory Array 1 is higher than that of the corresponding cell in Memory Array 2, the output bit is assigned a digital '1'; otherwise, it is assigned a digital '0'. The use of two arrays increases the unpredictability of the PUF response, thereby enhancing the overall security.

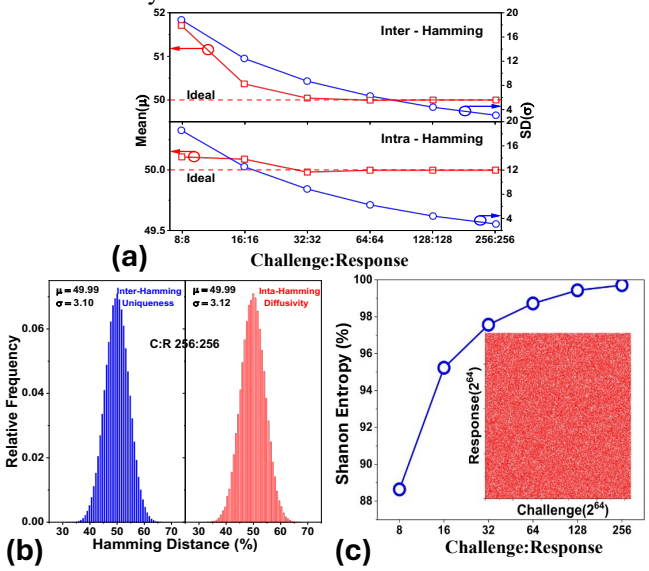

Fig. 6 (a) Inter- and intra-Hamming distances tend towards idealized values (μ = 50% and small σ) for pulsed biasing with increasing CRPs. (b) Uniqueness (inter-Hamming distance) and diffusivity (intra-Hamming distance) for 256:256 CRPs. (c) Unpredictability of response measured using Shannon entropy, inset: Spectral patterns of all 64:64 CRPs (on 2^{21} pairs), showing no visual correlation (unpredictable)

First, we evaluate the inter and intra-Hamming distance and verify that the PUF characteristics tend to the idealized values (μ ~ 50% and smaller σ) with increasing CRPs [Fig.6(a)]. Next, we evaluate the uniqueness and diffusivity for PUFs, by extracting the inter- and intra-Hamming distance [Fig.6(b)] (μ~50% and σ~3% for 256:256 CRP). These results predict enhanced performance compared to experimental results for similar response bits [6,7]. Finally, we evaluate the unpredictability of the PUF using Shannon entropy (V_p = 2.25 V, t_{pw} = 50 μs) [Fig. 6(c)]. As the number of response bits increases, the entropy value moves closer to the ideal value of 100%, indicating a highly random and unpredictable response across CRPs. To further support this, the inset of [Fig. 6(c)] shows the spectral map of 256:256. The absence of significant visual patterns illustrates that the responses are inherently random and uncorrelated. After generating the PUF response matrix, the randomness of the output bits was evaluated using the NIST SP 800-22 statistical test suite. A P-value represents the probability that a truly random sequence would produce a result less random than the tested sequence. According to the criteria, a P-value greater than 0.01 indicates that the test has passed. The proposed PUF architecture successfully passed all 16 tests [Table 1], confirming that the generated response exhibits high randomness [8].

Tests	P-Value	Result
Frequency	0.534146	**Pass**
Block Frequency	0.534146	**Pass**
Cumulative Sums (F)	0.739918	**Pass**
Cumulative Sums (R)	0.739918	**Pass**
Runs	0.350485	**Pass**
Longest Run	0.534146	**Pass**
Rank	0.991468	**Pass**
FFT	0.739918	**Pass**
Overlapping Template	0.350485	**Pass**
Universal	0.534146	**Pass**
Approximate Entropy	0.066882	**Pass**
Serial	0.516869	**Pass**
Linear Complexity	0.008879	**Pass**
Non-overlapping Template	0.458603	**Pass**
Random Excursions	0.457939	**Pass**
Random Excursions Variant	0.626478	**Pass**

Table 1: Evaluation of PUF Output Randomness Using NIST SP 800-22 Statistical Tests

V. CONCLUSIONS

We demonstrate MoS_2-based RRAMs as promising candidates for hardware security by leveraging stochastic switching and tunable variability. Our kMC simulations, calibrated with experimental data, show large control over HRS resistance under DC and pulsed biasing. By varying pulse parameters (V_p, t_{pw} and N_p), the statistical parameters of the HRS distribution mean and coefficient of variance tuned over six (10^3 to 10^9 Ω) and three (10^{-2} to 10^1) orders of magnitude, respectively. This enables a robust PUF design, validated through inter/intra-Hamming distance analysis, spectral mapping, and successful completion of the NIST SP 800-22 statistical test suite.

REFERENCES

[1] Cao Y, Liu W, Qin L et al. Entropy 2022; 24: 1566.
[2] Zahoor F, Hussin FA, Isyaku UB et al. Discover Nano 2023; 18:36.
[3] Mitra S, Kabiraj A, Mahapatra S. NPJ 2D Mater Appl 2021; 5:33.
[4] Peddaboina L, Agrawal K, Kumar P, Hegde G, Badami O, Bhattacharjee S. Adv Theory Simul 2025;
[5] Bhattacharjee S, Caruso E, McEvoy N et al. ACS Appl Mater Interfaces 2020; 12: 6022–6029.
[6] Lin B, Pang Y, Gao B et al. IEEE J Solid-State Circuits 2021; 56: 1641–1650.
[7] Liu R, Wu H, Pang Y, Qian H, Yu S. 2016 IEEE International Symposium on Hardware Oriented Security and Trust (HOST), IEEE 2016, 13–18.
[8] Rajendran G, Zahoor F, Thakker SS et al. 2024 37th International Conference on VLSI Design and 2024 23rd International Conference on Embedded Systems (VLSID), IEEE 2024, 560–564.

ACKNOWLEDGEMENTS

S.B. acknowledges project funding support from ANRF (erstwhile SERB) grant no. SRG/2022/000441 and BRNS-YSRA grant.no 58/20/01/2024-BRNS.